YMTHE, Volume *28*

Supplemental Information

In Vivo Generation of CAR T Cells Selectively in Human $CD4^+$ Lymphocytes

Shiwani Agarwal, Julia D.S. Hanauer, Annika M. Frank, Vanessa Riechert, Frederic B. Thalheimer, and Christian J. Buchholz

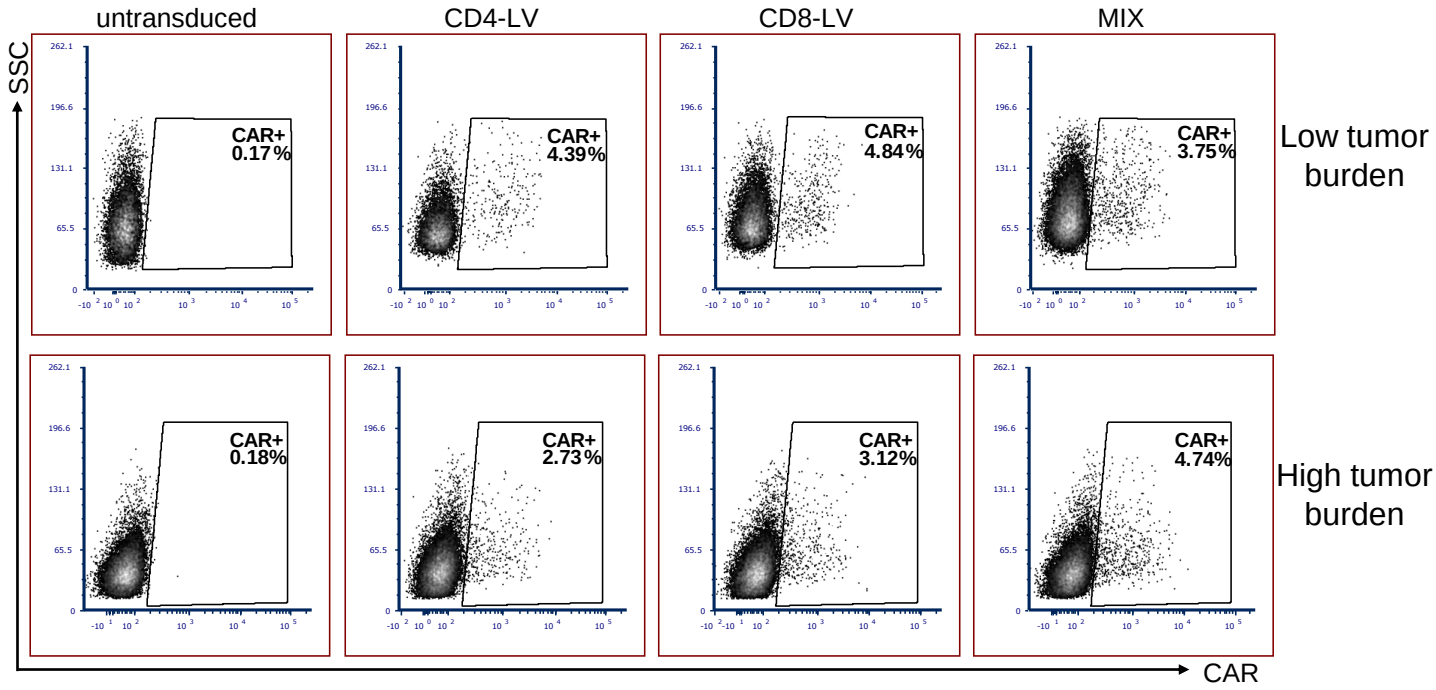

Figure S1: CAR expression at the start of *in vitro* repetitive killing assay

FACS plots displaying CAR expression gated on CD4+, CD8+ and CD3+ populations respectively, analyzed at day 0 of the repetitive killing assay shown in Fig. 1D-E.

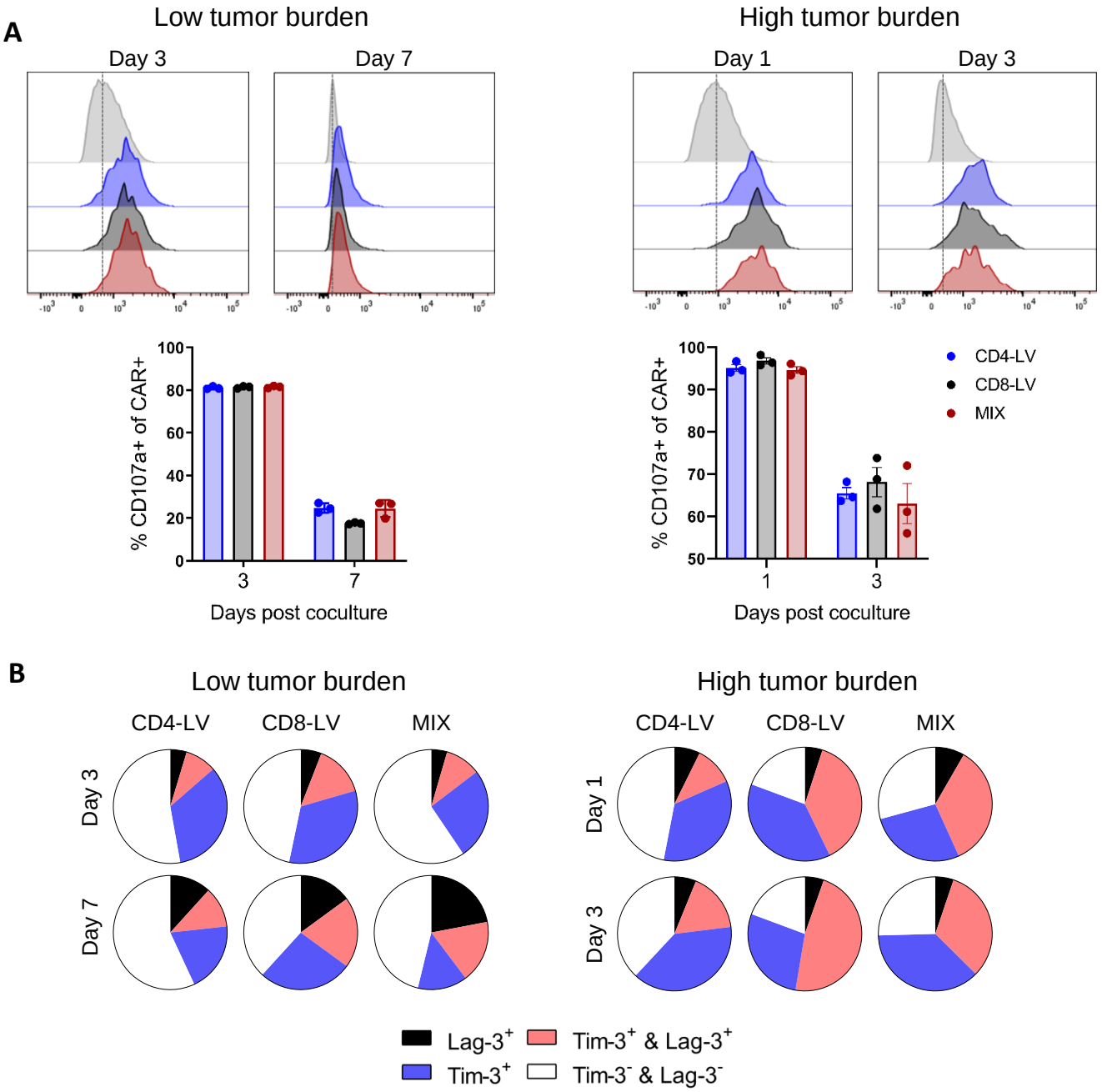

Figure S2: Inhibitory receptor and CD107a expression

(A) Histograms and bar diagrams of CD107a expression and **(B)** graphical representation of inhibitory receptors Lag-3 and Tim-3 on CAR+ T cells gated on CD4+, CD8+ and CD3+ populations respectively, analyzed at day 1, 3 and 7 post coculture of repetitive killing assay of low and high tumor burden (Fig. 1D-E).

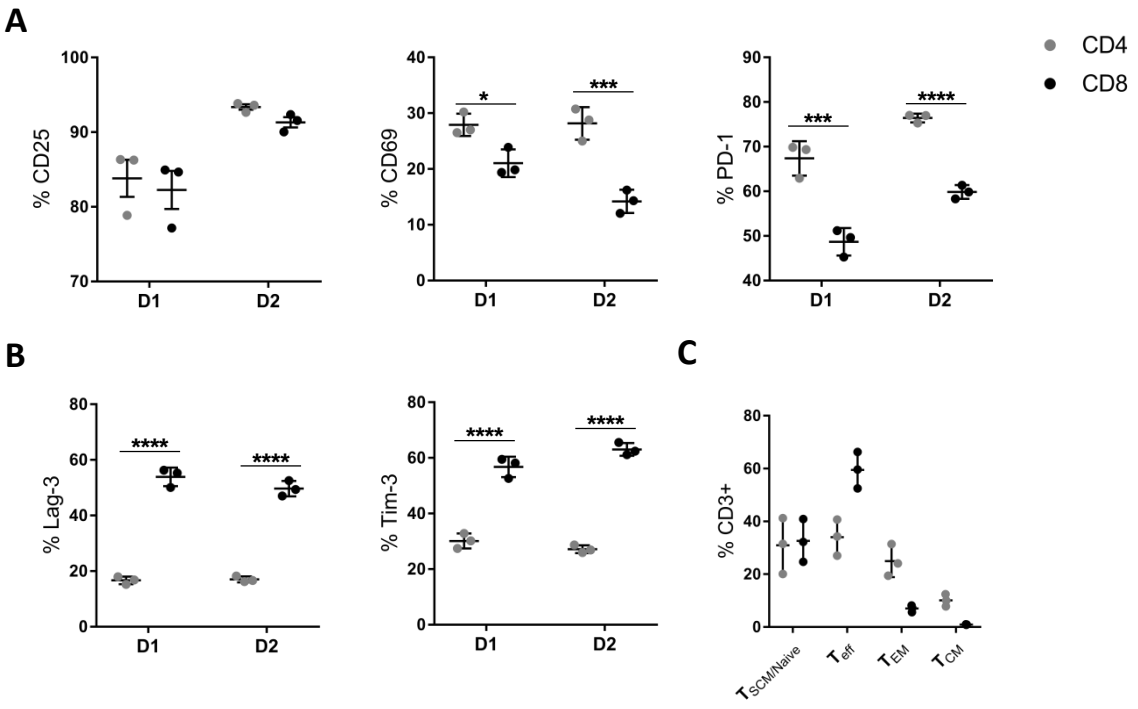

Figure S3: CD8+ T cells display an activation-induced exhausted phenotype

Human PBMC from two donors (D1 and D2) were activated with plate-bound anti-CD3 and anti-CD28 supplemented with IL-2 for 3 days. CD4+ (grey circles) and CD8+ (black circles) fractions were compared for their activation profile based on CD25, CD69 and PD-1 **(A)**, exhaustion profile based on Lag-3 and Tim-3 expression **(B)** and memory phenotype based on CD45RA and CD62L expression **(C)** 3 days post activation by FACS.

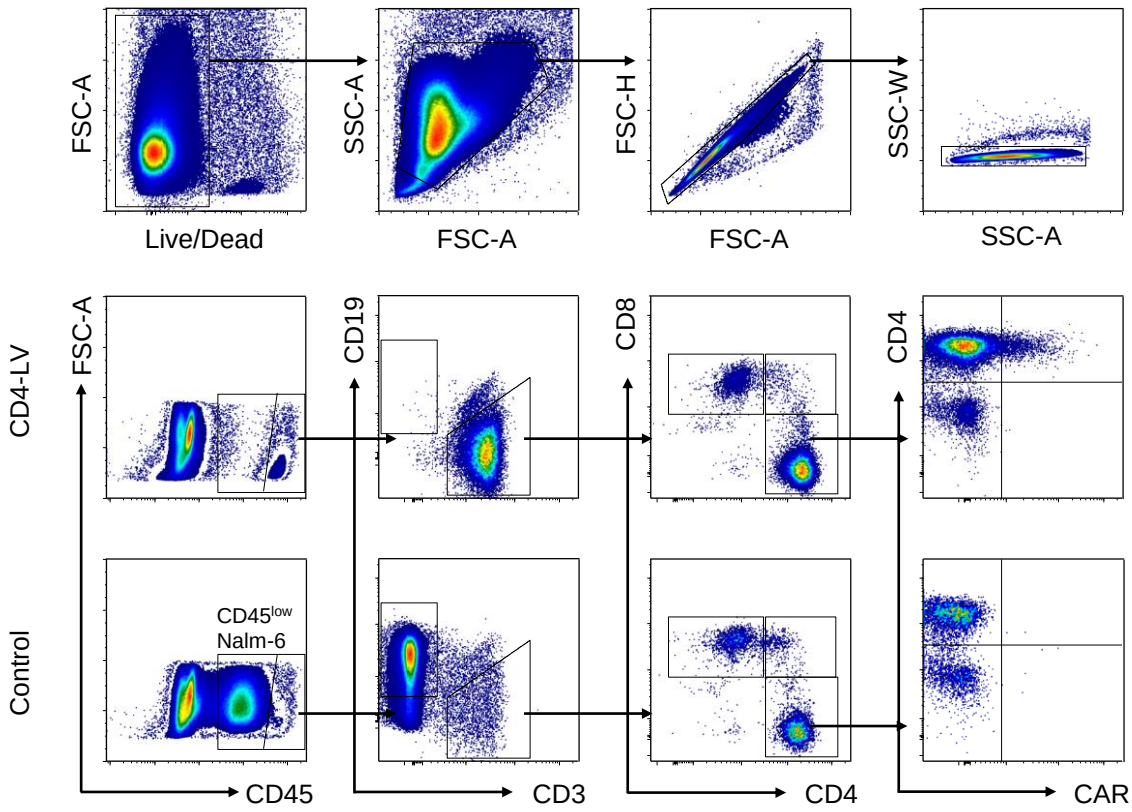

Figure S4: Gating strategy for tumor model

Human cells were identified as living single lymphocyte population that expresses CD45. Cells within the CD45 gate were further gated for CD3 and CD19 populations. Cells within the CD3 gate were gated for human CD8, CD4 and double positive. Further, from the CD4 or CD8 gate CAR positive cells were gated in the different vector groups.

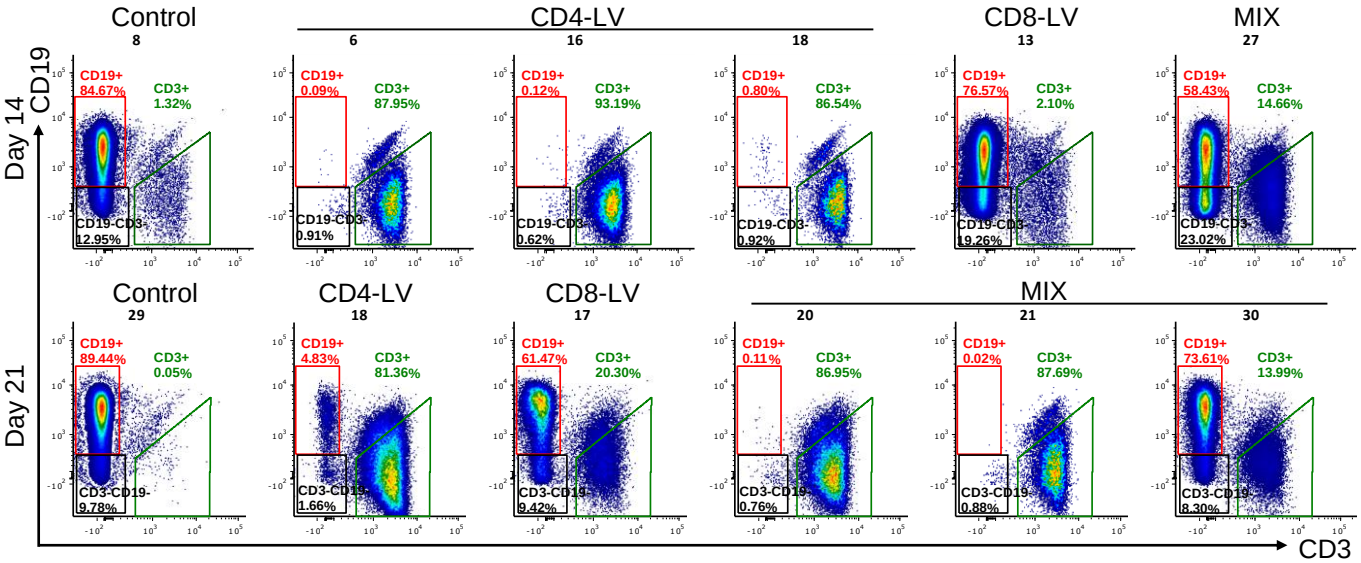

Figure S5: No loss of CD19 expression in Nalm6 cells *in vivo*

Bone marrow cells harvested at day 14 and day 21 from mice of the indicated treatment groups according to Fig. 3 were analyzed by flow cytometry for the presence of CD19-negative Nalm6 cells. Cells were pre-gated on CD45+ population according to Fig. S4. Mice which cleared CD19+ tumor cells (red box) also showed absence of CD3-CD19- cells (black box).

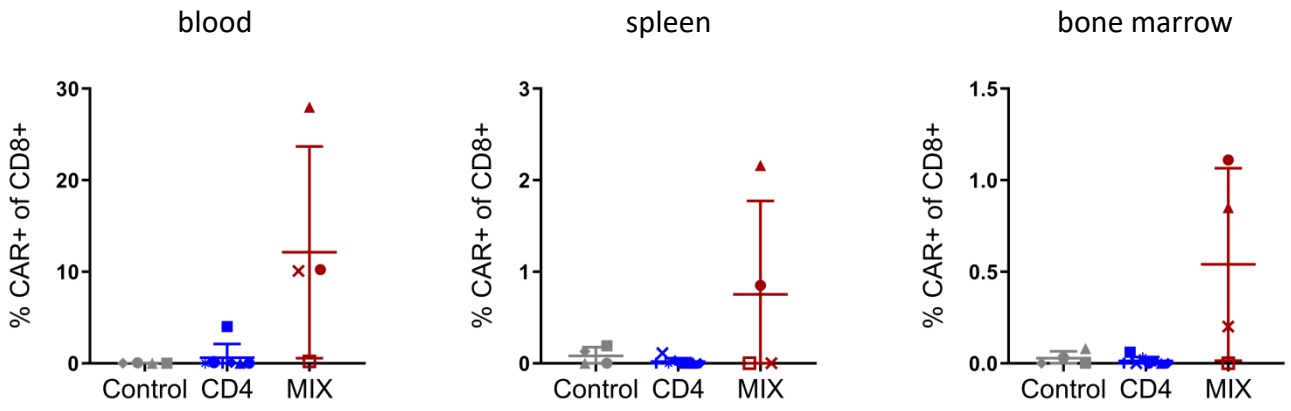

Figure S6: CD8+ CAR T cells in huNSG mice

Cells isolated from the blood, spleen and bone marrow of mice shown in Fig. 5 were evaluated by flow cytometry for the percentage of CAR+ cells within the CD8+CD3+ fraction.

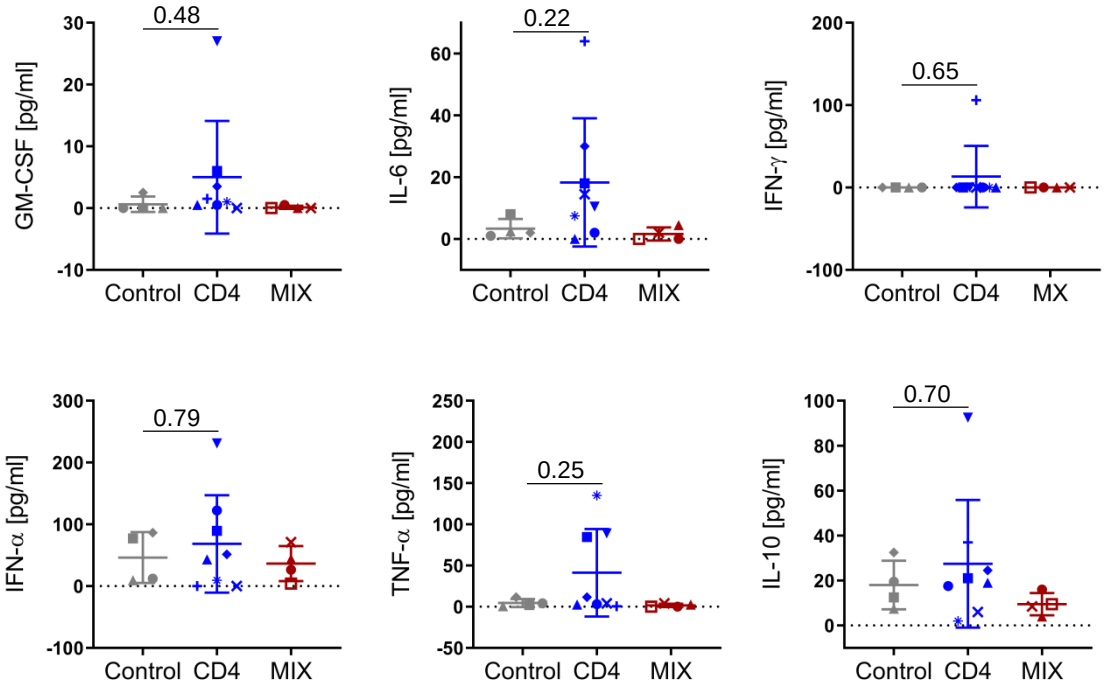

Figure S7: Cytokine levels in humanized mice

Cytokine levels in plasma obtained at final sacrifice of each individual mouse. Every symbol indicates a distinct mouse and is identical to the symbols used in Fig. 5 and 6. Mean ± SEM of n = 2 technical replicates.

Supplemental Table 1: CD4 T cell phenotype

		Tbet (Th1)	Gata-3 (Th2)	RORγt (Th17)	FoxP3 (Treg)
Control	**CD4+CAR-**	30.96 ± 5.72	49.82 ± 4.15	18.01 ± 2.25	1.20 ± 0.22
Vector	**CD4+CAR-**	43.30 ± 6.59	37.47 ± 6.53	18.94 ± 5.83	0.28 ± 0.06
	CD4+CAR+	40.89 ± 12.24	38.16 ± 11.18	20.73 ± 9.15	0.20 ± 0.04

Supplemental Table 2: Vector doses administered *in vivo*

Mice	Experiment	Vector particles injected/mouse		Gene transfer units (t.u.)/mouse	
		CD4-LV	CD8-LV	CD4-LV (A301)	CD8-LV(Molt4)
NSG	Fig. 2	4×10^{10}	-	2×10^{6}	-
	Fig. 3	1×10^{11}	2.5×10^{11}	2×10^{6}	3.6×10^{6}
huNSG	Fig. 5	4×10^{10}	7×10^{11}	2×10^{6}	2.9×10^{6}